Journal of Physics:
Conference Series

Porosity determination in doped graphites using small-angle neutron scattering measurements

Porosity determination in doped graphites using small-angle neutron scattering measurements

K Mergia[1], K L Stefanopoulos[2], M Martinez-Escandell[3] and Pavel Strunz[4]

[1] Institute of Nuclear Technology and Radiation Protection, National Centre for Scientific Research "Demokritos", GR-15310 Aghia Paraskevi Attikis, Greece
[2] Institute of Physical Chemistry, National Centre for Scientific Research "Demokritos", GR-15310 Aghia Paraskevi Attikis, Greece
[3] Department of Inorganic Chemistry, University of Alicante, E-03690 Alicante, Spain
[4] Nuclear Physics Institute, Neutron Physics Laboratory, CZ-25068 Řež near Prague, Czech Republic

E-mail: kmergia@ipta.demokritos.gr

Abstract. The porosity of undoped and Zr- and Ti-doped graphites has been determined using small-angle neutron scattering measurements. To differentiate between open and closed pores in the neutron scattering measurements the contrast matching technique was employed. In the pore volume distribution three distinct sizes of pores are present. Doping increases the volume fraction of pores, shifts the mean size to lower values and makes the size distributions wider. In addition it enhances drastically the closed porosity.

1. Introduction

Carbon and graphite are attractive materials for high-temperature applications due to their high thermal conductivity, low electrical resistivity, high strength, high modulus, excellent thermal shock resistance and light weight. They are widely used as engineering materials, such as heaters, electrical contacts, high-temperature heat exchangers, rocket nozzles, leading edges of aircraft wings and plasma facing materials in fusion devices etc. [1-3]. For Fusion application the main drawback of carbon-based materials is their chemical erosion under hydrogen bombardment which has to be avoided [4-5]. Doping of carbon with small amounts of certain elements is known to improve its properties. High thermal conductivity and high thermal shock resistance, [6-7] and elimination or reduction of their chemical erosion are achieved [8-9] through doping. Some dopants, such as TiC, present catalytic effects on the graphitization, leading to a higher degree of graphitization and thus enhancement of thermal conductivity. In addition, they may act as reinforcement improving the mechanical properties [10]. For an effective improvement of all the properties, a very fine and homogeneous dispersion of the dopants is required, since both the thermo-mechanical properties and the reduction of chemical erosion are particularly sensitive to the particle size of the dopants [8].

The production of doped-carbon materials via co-pyrolysis of a carbon precursor with a heteroatom source soluble in the carbon precursor is a good alternative to produce doped self-sintering carbon with a homogeneous particle distribution. This material can be used to produce graphites without the

need of using a binder. The heteroatom precursor must be soluble in the carbon source (usually carbon or petroleum pitch) in order to achieve a good dispersion of the dopant.

A number of methods have been applied for the investigation of the porosity in carbon. Among these are gas adsorption [11], mercury intrusion porosimetry [12], TEM [13] and small-angle scattering techniques [14-17]. Gas adsorption and mercury porosimetry do not provide information about closed porosity and TEM only gives limited information concerning pore connectivity. Small-Angle Neutron Scattering (SANS) can provide information for both open and closed porosity.

In the current work we present a SANS study of the pore microstructure in samples of doped and undoped graphites with the aim to elucidate the effect of doping on the porosity. Three types of dopants were used, namely a) Ti in the form of TiC nanoparticles, b) Ti using as a precursor tetrabutyl-ortotitanate and c) Zr using as a precursor zirconium acetyl acetonate. Closed and open porosity have been determined using the contrast variation technique [18]. The volume distribution, average size and specific surface area (SSA, i.e. surface area per unit volume) of the pores in these materials have been determined.

2. Experimental

2.1 Sample fabrication

Titanium doped mesophase pitches were prepared by co-pyrolysis of an aromatic petroleum residue (ethylene tar) with two different titanium sources, tetrabutyl-ortotitanate and titanium carbide nano-powder with sizes around 100 nm. In the case of zirconium doped mesophase pitches, zirconium acetyl acetonate was used as Zr-precursor. The mixture of petroleum residue with the titanium or zirconium compound was prepared in an ultrasonic bath. Pyrolysis of the mixtures was carried out in a laboratory pyrolysis plant using 350 g of mixture in the reactor. Pyrolysis was performed at 440ºC, soak time 4 h and 1 MPa pressure. A reference sample without the titanium or zirconium compound was also prepared.

Self sintering mesophase powders containing Ti or Zr were prepared by extraction of the mesophase pitch, obtained in the pyrolysis, with tetrahydrofurane at its boiling point for 2 hours. This step was necessary to reduce the amount of volatile matter produced during heat-treatment of these self-sintering powders. In order to optimise the self-sintering abilities of the extracted materials and to improve the properties of the resulting graphites, a stabilisation stage has been carried out. All stabilisations were carried out at 175 ºC, using dry air (100 mL/min), a heating rate of 2 ºC/min and soaking time varying from 0 to 2 hours. All the stabilised samples were sieved to particle size smaller than 63 μm.

Table.1. Sample description.

Sample Code	Precursor	Dopant	Amount of metal in graphite (at%)	Open Porosity, $P_{O,im}$ (%)
C	none	none	0	4
C/Tin	TiC nanoparticles	Ti	2.4	2
C/Tib	Tetrabutyl-ortotitanate	Ti	2.2	6
C/Zr	Zr acetyl acetonate	Zr	1.4	6

Three grams of self sintering powder were uniaxially pressed at room temperature, at 175 MPa, to prepare green compacts of 5×10×50 mm. The compacts were heat treated under nitrogen flow of 60ml/min to 1500 ºC, heating rate 1.0 ºC/min, and further high-temperature treated at 2600 ºC (10 ºC/min) under inert atmosphere.

Table 1 describes the samples investigated in the current study and also the values of open porosity as measured by immersion of the bulk samples in the water are given.

2.2 SANS measurements

The theory of small-angle scattering is well described in the literature both generally [19, 20] and specifically for applications in porous materials [16, 21-22]. SANS with the utilization of the "contrast matching" technique has been used to determine both open and closed porosity in carbon and chars [14-17, 22-24].

In a SANS experiment the absolute neutron scattering cross section, $I(Q)$, is recorded as a function of the scattering vector $Q = 4\pi \sin\theta / \lambda$ where 2θ is the scattering angle, i.e. the angle between the incident and the scattered neutron beam and λ the neutron wavelength. SANS arises from the neutron scattering length density difference, $\Delta(SLD)$, between the matrix and inhomogeneities e.g. precipitates, pores. The neutron scattering length of the matrix, SLD_M, is given by

$$SLD_M = \frac{\rho_{sk} N_{Av}}{MB} \sum_i c_i b_i = C \rho_{sk} \quad (1)$$

where MB the average molecular mass, N_{Av} the Avogadro number, b_i is the neutron scattering length of element i with atomic concentration c_i and the sum is over all the elements present in the matrix. It should be noted that in equation (1) the constant C is known from the chemical composition of the matrix and the tabulated values of b_i, whereas the skeleton density ρ_{sk} has to be measured or assumed from the crystallographic structure. If we assume that the material density within the pores is very low then $\Delta(SLD) = SLD_M - SLD_{\text{pore}} \cong SLD_M$.

The SLD_M values as calculated vary between 5.99×10^{-6} (Zr doped sample) and 6.39×10^{-6} Å^{-2} (Ti doped sample using TiC nanoparticles). For the undoped sample the SLD_M value (6.70×10^{-6} Å^{-2}) is about 4% higher than that of D_2O. Therefore for the undoped sample 100% D_2O was used for the contrast matching.

Specimens for the SANS measurements were prepared by grinding the initially received samples to a powder of grain sizes larger than 40 μm. Two set of experiments were performed at room temperature, the called "dry" and "wet" sample measurements. In the "dry" sample measurements the neutron scattering measured from the powdered sample arises from both open and closed pores, whereas in the "wet" sample the neutron scattering arises from the closed pores. 1 mm thick Hellma cuvettes were used as sample holders. As a contrast matching liquid D_2O/H_2O was used and the concentration of D_2O/H_2O was calculated such as to match the SLD_M of the respective sample.

In the "wet" sample measurements, the sample powder was immersed in a H_2O/D_2O mixture which had the same neutron scattering length density as that of the solid ("contrast matching"). The pores accessible from the grain surface are filled with the liquid and since the neutron scattering length density difference of these filled pores with the matrix is zero, only SANS from the unfilled (closed) pores is received. The "wet" samples mixed with D_2O/H_2O were allowed for about 4 h to come to equilibrium before measurement. Some "wet" samples were re-measured after 24 h to see if there was any effect of the water wettability but no differences were observed in the values of the scattering at the different Q-values (i.e. scattering curves coincided within statistical errors).

The SANS scattering data were corrected for sample thickness, transmission and instrumental resolution and they were scaled to yield absolute cross sections.

The SANS measurements were carried out at the neutron double-crystal diffractometer MAUD (formerly DN-2) at NPI Řež (λ=0.209 nm) [25]. The measured intensity at a double-crystal diffractometer corresponds to the differential SANS cross section of the sample integrated in the vertical direction and smeared by the resolution function in the horizontal direction. The shape of the

horizontal resolution function is equivalent to the shape of the curve measured without the sample. The MAUD instrument is tuned to operate over two ranges of the scattering vector: 2.6×10^{-3} to 0.022 nm^{-1} and 0.014 to 0.12 nm^{-1}. An absolute calibration of scattering cross-sections was performed by measuring the intensity of the direct beam.

The SANS data were fitted using SASProFit software [26] based on indirect Fourier transformation method [27]. In the data treatment it was assumed that the sample is composed of a polydisperse distribution of spherical scatterers. From the numerical processing of the measured cross sections [25] the pore volume distribution, $\varphi(R)$, the porosity, the pore mean size and the pores specific surface area are determined. From the "dry" sample measurements the total porosity parameters are determined whereas from the "wet" sample measurements only the closed porosity ones.

3. Results and Discussion

3.1 SANS results

Figure 1 presents the scattering factor from "dry" and "wet" samples. Two Q ranges have been measured with low and high resolution. The non-exact overlap of the two ranges is caused by the different resolution functions. For low resolution, much broader (angularly) instrumental curve is used than for the high resolution. The solid lines in Figure 1 are fitted curves to the data points and they have been derived using the procedure described in [26].

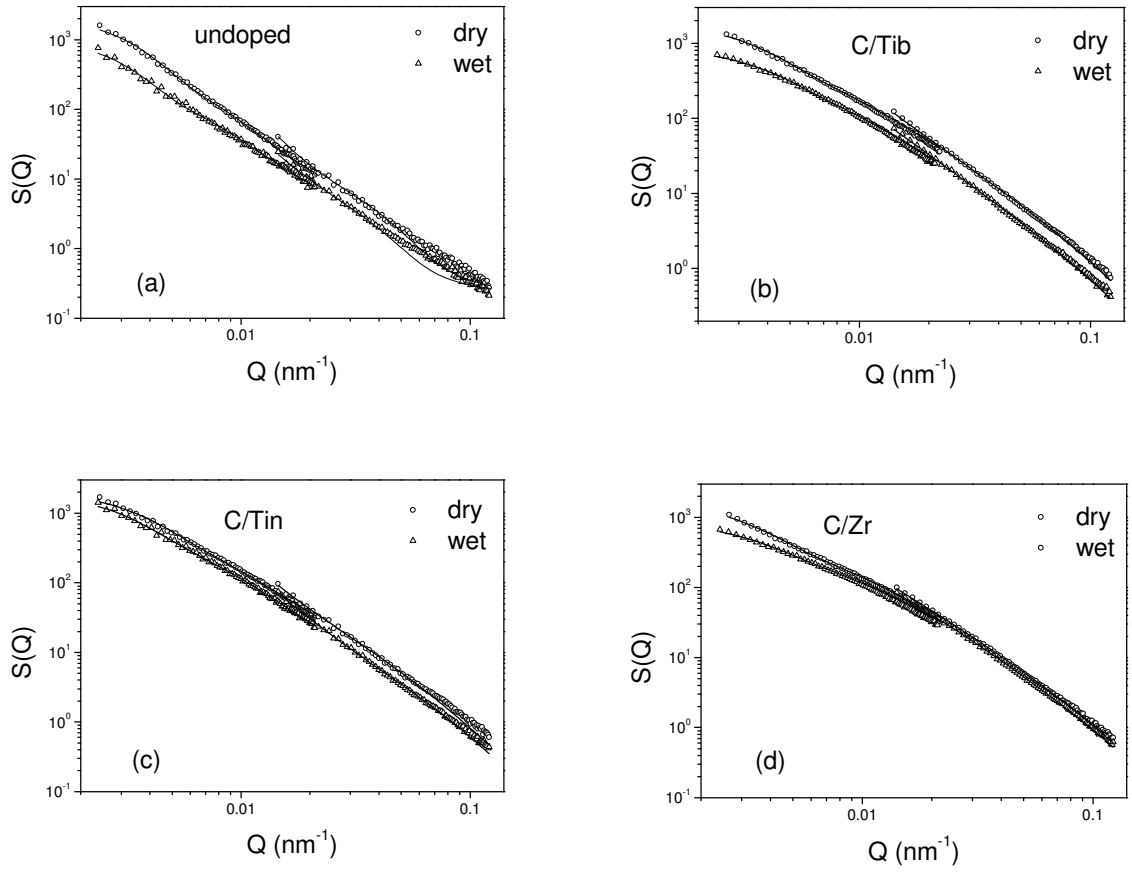

Figure 1. Scattering factors for the "dry" and "wet" samples: (a) undoped, (b) C/Tib, (c) C/Tin and (d) C/Zr. Solid lines are fitted curves to the data according to [26].

The scattering curves have very similar shapes for all the doped samples and in both "dry" and "wet" sample measurements and differ from those of the undoped sample. This observation demonstrates that the morphology and size distributions of open ("dry") and closed ("wet") pores are very similar and that the different dopants introduce similar changes with respect to the undoped sample. However, the absolute scattering cross section diversity among the different samples reflects the different values of either total or closed porosity. For the undoped samples the absolute intensity of the "wet" sample is about half that of the "dry" one which implies that of the total porosity half of it is closed. A similar reduction occurs for the C/Tib sample. On the contrary for the C/Tin sample the absolute intensity of the "wet" sample decreases by about 20% which implies that 20% of the porosity is open (figure 1c). For the Zr doped sample the absolute intensity decreases by about 40% (figure 1b).

From the numerical processing of the data the pore volume distribution, $\phi(R)$, was determined, for the "dry" and "wet" samples, which corresponds to total and closed porosity, respectively. The volume distribution for total and closed pores is depicted in figures 2 and 3, respectively. From these figures it is apparent that the doping does not affect the morphology of the volume distributions, but shifts the volume distribution to smaller sizes. In all samples the volume fraction distribution is trimodal. Doping generally increases the volume fraction of pores, shifts the mean size to lower values and makes the size distributions wider. For the total porosity the first size region is centered around 25 nm, the second around 160 nm and the third around 600 nm. Similar features are present in the size distribution of closed pores.

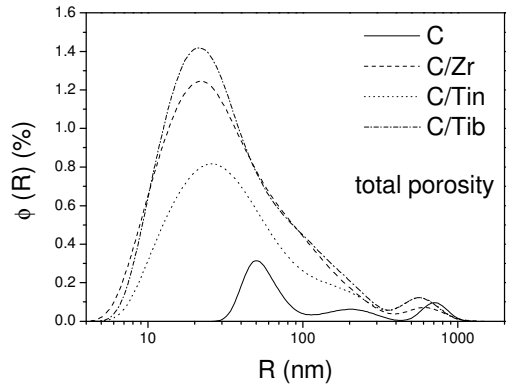

Figure 2. Volume distribution of total pores.

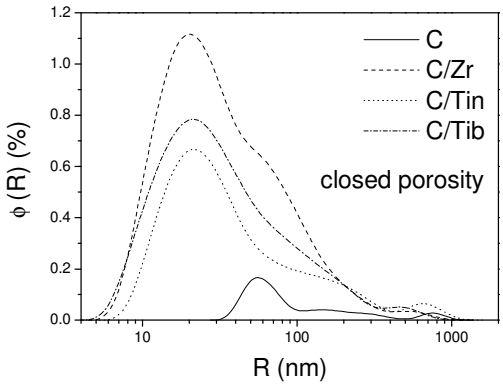

Figure 3. Volume distribution of closed pores.

In all the samples, except the C/Tin, the dopant was introduced chemically and thus the observed SANS arises solely from open or closed porosity. In the C/Tin sample the doping was made using TiC nanoparticles having an average size of 100 nm and volume fraction of about 4%. Therefore, it would be expected the presence of TiC nanoparticles to emerge in the volume distributions of C/Tin sample in both figures 2 and 3. Such a presence of the TiC is not at all obvious taking into account that the volume fraction of the incorporated nanoparticles of around 4% is much larger than the volume fraction at the peak of the distribution. Moreover, it is observed that the volume fraction of the C/Tin sample at around 10 nm is lower than that of the other doped samples. Therefore it is concluded that the TiC nanoparticles after the thermal processing have been dissolved in the matrix and no TiC agglomerates in a large extent remain.

From the size distribution the average radius of total and closed pores are determined (see table 2). As it can be seen, the doping reduces drastically the average size of the pores either open or closed with the maximum reduction observed for the Zr doped sample of about 70%.

Concerning the porosity values, it is observed that there is a drastic increase of the total porosity in the doped samples and this actually reflects the corresponding increase of the closed porosity. The closed porosity of the two Ti doped and the Zr doped samples compared to the undoped one is about three times larger. The sample doped with Tetrabutyl-ortotitanate has the largest total porosity. The dopant either Zr or Ti seems causes a four-fold increase of the closed porosity, whereas the open porosity remains almost the same as in the undoped sample except for the case of C/Tib.

Table 2. Pore size parameters determined from SANS data.

Sample	P_T	Total porosity SSA	$\langle R_T \rangle$ (open+closed)	P_C	Closed porosity SSA	$\langle R_C \rangle$ (close)	P_O
	(%)	($\times 10^3$ cm^{-1})	(nm)	(%)	($\times 10^3$ cm^{-1})	(nm)	(%)
C	5.4 ± 0.1	8.9 ± 0.4	500 ± 20	2.5 ± 0.1	8.9 ± 0.7	487 ± 38	2.9
C/Tin	13.0 ± 0.2	51.3 ± 1.4	300 ± 6	9.3 ± 0.2	37.3 ± 2.1	313 ± 9	3.7
C/Tib	17.1 ± 0.2	83.0 ± 3.2	244 ± 7	9.2 ± 0.1	49.6 ± 1.8	180 ± 4	7.9
C/Zr	14.7 ± 0.2	77.9 ± 3.0	221 ± 5	11.4 ± 0.2	67.0 ± 2.2	156 ± 3	3.3

The open porosity values differ from those determined by the immersion of the bulk samples in water from about 24% (C/Tib sample) up to 82%(Ti/Zr sample). This can be understood as follows. In a macroscopic sample (mm dimensions) there are two possibilities. Either a) all the network paths for each μm region (open grain porosity) are interconnected and terminate to the surface of the macroscopic sample (percolation) or b) only part of the network paths are interconnected and terminate to the surface. For the former case the open and consequently also the closed porosity values for the grain and the macroscopic sample will be the same. In the second case, if we grind the samples into grains, as it is done for the SANS measurements, more networks are exposed to the grain surface making the grain open porosity higher than that of the bulk sample [17]. The SSA for the total porosity increases with doping by a factor varying between 5.7 (C/Tin) and 9 (C/Tib, C/Zr) (table 2). For the closed porosity SSA is four (C/Tin) up to 7.5 times (C/Zr) higher than that of the undoped sample. The increase of the pore surface with doping is expected since the average size decreases and the volume fraction of pores increases with doping.

4. Conclusions

SANS measurements with contrast matching have been employed to determine the open and closed porosity in doped and undoped graphites. It is concluded that the volume distribution of the pores is very similar for all the doped samples and for either closed or open pores. In the volume distribution three distinct sizes of pores are present. Doping with either Zr or Ti decreases the average pore size but increases strongly the closed porosity values. Also in the doped samples the SSA of the closed pores increases drastically with respect to the undoped ones. In conclusion doping introduces microstructural changes which are manifested by the change in the pore volume distribution and closed porosity values.

Acknowledgements

This work has been carried out within the framework of the Integrated European Project "ExtreMat" (contract NMP-CT-2004-500253) with financial support by the European Community. This paper only reflects the views of the authors and the European Community is not liable for any use of the information contained therein. The support of the European Commission through the research project with Contract No. RII3-CT-2003-505925 (NMI3) is acknowledged.

References

[1] Fitzer E 1987 *Carbon* **25** 163

[2] Blazewicz S, Blocki J, Chlopek J, Godlewski J, Mickalowski J, Pakonski K, Piekarczyk J and Stodulski M 1996 *Carbon* **34** 1393
[3] Qian J P, Liu X, Li P Y and Guo Z 1992 *J. Nucl. Mater*. **191-194** 340
[4] Roth J, García-Rosales C 1996 *Nucl. Fus*. **36** (1996) 1647. Corrigendum 1997 *Nucl. Fus*. **37** 897
[5] Vietzke E and Haasz A A 1996 *Physical Processes of the Interaction of Fusion Plasmas with Solids* ed Hofer W O and Roth J (Academic Press) p 135
[6] Marinkovich S 1984 *Chemistry and Physics of Carbon* vol. 19 ed Thrower P A (New York: Marcel Decker) p 416
[7] Ogawa I, Kobayashi K and Nishikawa S 1988 *J. Mater. Sci*. **23** 1363
[8] García-Rosales C and Balden M 2001 *J. Nucl. Mater*. **290-293** 173
[9] Starke P, Fantz U and Balden M 2005 *J. Nucl. Mater*. **337–339** 1005
[10] Qiu H, Han L and Liu L 2005 *Carbon* **43** 1021
[11] Cregg S J and Sing K S W 1982 *Adsorption, Surface Area and Porosity* (New York: Academic Press)
[12] Zgrablich G, Mendioroz S, Daza L, Pajares J, Mayagoitia V, Rojas F and Conner W C, 1991 *Langmuir* **7** 779
[13] Huxham I M, Rowatt B, Sherrington D C and Tetley L 1992 *Polymer* **33** 2768
[14] Kostorz G 1979 Neutron scattering *Treatise on materials science and technology* ed Kostorz G (New York: Academic Press) vol 15 p 227
[15] Porod G 1982 *Small-angle X-ray scattering* ed Glatter O and Kratky O (New York: Academic Press) p 17-62
[16] Calo J M and Hall P J 2004 *Carbon* **42** 1299
[17] Mergia K, Stefanopoulos K L, Ordás N and García-Rosales C (2010) *Microporous and Mesoporous Materials* **134** 14
[18] Stuhrmann H B and Miller A 1978 *J. Appl. Cryst*. **11** 325
[19] Guinier A and Fournet G 1995 *Small-Angle Scattering of X-rays* (New York: John Wiley)
[20] Lindner P and Zemb T 1991 *Neutron, X-ray and Light Scattering* (Amsterdam: Elsevier)
[21] Schmidt P W 1991 *J. Appl. Cryst*. **24** 414
[22] Calo J M, Hall P J and Antxustegi M M 2001 *Colloids & Surfaces A*: *Physicochem. Eng. Aspects* **187-188** 219
[23] Gethner J S 1986 *J. Appl. Phys*. **59** 1068
[24] Hall P J, Antxustegi M M and Calo J M 1998 *Energy Fuels* **12** 542
[25] Strunz P, Šaroun J, Mikula P, Lukáš P and Eichhorn F *1997 J. Appl. Crystallogr*. **30** 844
[26] Šaroun J *2000 J. Appl. Cryst.* **33** 824
[27] Glatter O 1977 *Acta Phys. Austr.* **47** 83